

Abstracts and Programme
Poster Presentations
EUROCARBON 2000
1st World Conference on Carbon
9 - 13 July 2000, Berlin

VOLUME II
ISBN 3-925543-16-3

In situ CONDUCTION ELECTRON SPIN RESONANCE AND THEORETICAL STUDIES OF GRAPHITE INTERCALATION BY NITRIC ACID

A.M. Ziatdinov*, P.G. Skrylnik, and A.N. Krivoshei
Institute of Chemistry, Far Eastern Branch of the Russian Academy of Sciences.
159, Prosp. 100-letiya, 690022 Vladivostok, RUSSIA. E-mail: chemi@online.ru.

Keywords: graphite, intercalation compounds, ESR

INTRODUCTION

In spite of numerous publications devoted to studies of various aspects of graphite intercalation compounds (GICs) structure and properties, hitherto many aspects of mechanism of "guest" molecules intercalation into graphite have not received sufficient attention. CESR technique is one of the most powerful methods for studying the graphite intercalation process, because shapes and intensities of the CESR signal both from non-intercalated and intercalated regions of graphite plate vary strongly during the intercalation. However, because of difficulty of similar experiments only a few CESR studies of graphite intercalation process have been undertaken¹⁻⁵. But even in these cases, in consequence of presence of skin effect the interpretation of changing the graphite CESR signal during the intercalation process comes across greater difficulties. This paper is devoted to the results of an *in situ* CESR study of HNO₃ molecules intercalation into narrow HOPG slab (with basal plane width being comparable with the skin-depth δ_c governed by the graphite c-axis conductivity σ_c). The results of theoretical analysis of reasons for 1) step-wise evolution of the CESR signal intensity from intercalated part of HOPG slab and for 2) increase of graphite CESR signal linewidth at the process of intercalation, are also presented.

RESULTS AND DISCUSSION

The CESR spectrum of HOPG plate consists of single asymmetric line determined by Dyson⁶ mechanism. The spectrum is axial with respect to the c-axis and is characterized by $g_{\parallel}=2.0474\pm 0.0002$ and $g_{\perp}=2.0029\pm 0.0002$. The line asymmetry parameter, A/B, being determined

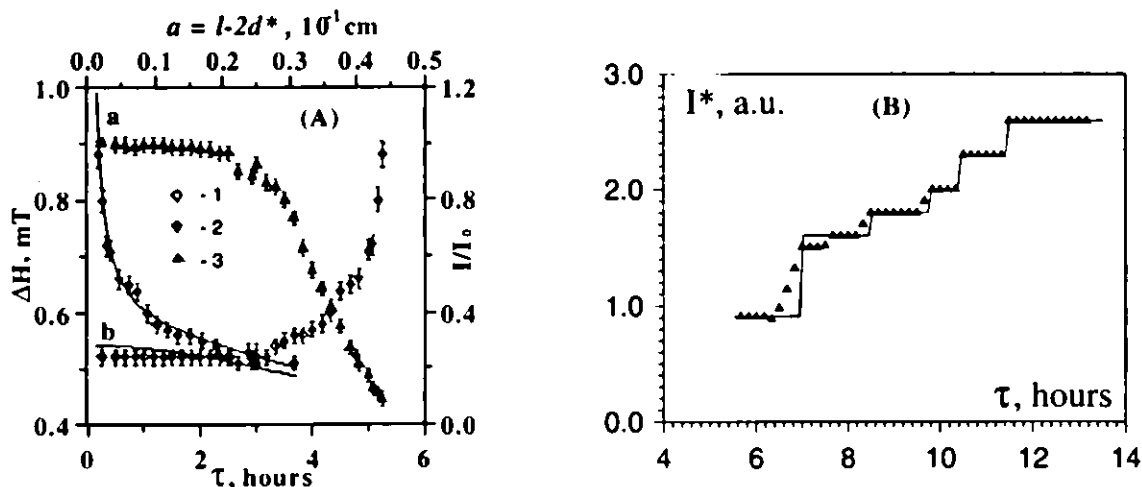


Fig. 1. Linewidth, ΔH (1, 2), and intensity, I (3), of graphite CESR signal (A), and intensity, I^* , of CESR signal of intercalated graphite (B), vs. exposure time, τ , in HNO₃ atmosphere. Solid lines are the theoretical data. In the left figure the line a (b) was calculated using the value of Dyson⁶ surface spin relaxation parameter $g = 1(0) \text{ cm}^{-1}$.

as the maximum/minimum peak height ratio, both measured with respect to the base-line of the first derivative of CESR absorption line, is 'normal' in the sense that the maximum peak height occurs at the lower magnetic fields and it is equal to ≈ 1.8 .

Several minutes after the injection of HNO₃ gas into the part of reactor with the HOPG plate, the CESR signal of graphite begins to transform and decrease in intensity until it fully disappears. Simultaneously, a new signal with $g_{\parallel}^* = 2.0019 \pm 0.0002$, and $g_{\perp}^* = 2.0030 \pm 0.0002$ appears in the spectrum.

The linewidth (the intensity), ΔH ($I = (A+B) \times \Delta H^2$), of the graphite CESR signal increases (decreases) vs. exposure time, τ , monotonously (Fig. 1A). The g_i ($i = \parallel, \perp$) values of graphite CESR signal do not change up to its disappearance.

Early in the development of the reaction, a wide scattering of the intensity, $I^* = (A^* + B^*) \times \Delta H^{*2}$, and the linewidth, ΔH^* , values of CESR signal with g_i^* has been observed. As the τ increases, this scattering decreases and both the $I^*(\tau)$ and $\Delta H^*(\tau)$ dependences take a well-marked step-wise form (Fig. 1B). The asymmetry ratio, A^*/B^* , and g_i^* -values of signal remain constant up to the end of reaction.

According to the X-ray diffraction data the first (last) 'plateau' in the Fig. 1B corresponds to the seventh (second) intercalation stage. For the proper description of the observed experimental dependence $I(\tau)$ analytical expressions for the stage fractions calculation by Kirczenow⁷ have been utilized. Then, with supposing chemical potential μ to be time dependent (by analogy with the Alstrom work⁸), we have obtained the step-wise dependence $I(\tau)$ (presented with solid line in Fig. 1B). However, we have found that simple relaxation function $\mu = \mu_{\infty}(1 - \exp(-\tau/\tau^*))$ adopted in ref.⁸ is, probably, a good approximation for large exposure time only. For the small time values μ increases approximately according to the power law. We suppose that slow increase in μ at the small τ may be accounted for by the considerable pristine graphite plate deformation required for the intercalation process to begin and by the large intercalant amount required for the formation of stages with low indices at the large time values.

The invariability of g_i and g_i^* ($i = \parallel, \perp$) values up to the disappearance of graphite CESR signal and the end of reaction, respectively, indicates that the boundary, which separates the intercalated and as-yet the non-intercalated parts of sample may be considered as non-conductive. We suppose that the reason for the significant broadening of the graphite CESR signal is the collisions of current carriers with this non-conductive boundary. Using the relation $d^* = (2D_{\text{int}} \times \tau)^{1/2}$ (where d^* is the thickness of the intercalated layer, $D_{\text{int}} = 7.2 \times 10^{-5} \text{ cm}^2 \cdot \text{cek}^{-1}$ is intercalate two-dimensional diffusion constant) the experimental dependence $\Delta H(\tau)$ (Fig. 1A) can be easily transformed into the dependence $\Delta H(a)$, where $a = l - 2d^*$ is the thickness of the non-intercalated part of HOPG plate (Fig. 1A). The latter dependence can be calculated theoretically as well, using the Dyson⁶ theory for the CESR in metals, including the effects of surface relaxation. It is shown in Fig. 1A, where the results of such analysis are presented, that the theoretical dependence of the graphite CESR linewidth, with Dyson⁶ parameter $g = 1 \text{ cm}^{-1}$ describes the experimental data well.

This work was partially supported by the Russian Foundation for Basic Research (grant No. 00-03-32610a).

REFERENCES

- (1) Davidov R., Milo O., Palchan I., and Selig H., *Synth. Met.*, 1983, 8, 83.
- (2) Palchan I., Davidov D., Zevin V., Polatsek G., and Selig H., *Phys. Rev.*, 1985, B32, 5554.
- (3) Palchan I., Mustachi F., Davidov D., and Selig H., *Synth. Met.*, 1984/1985, 10, 101.
- (4) Nakajima N., Kawamura K., and Tsuzuku T., *J. Phys. Soc. Jpn.*, 1988, 57, 1572.
- (5) Ziatdinov A.M., and Mishchenko N.M., *J. Phys. Chem. Solids*, 1997, 58, 1167.
- (6) Dyson F.J., *Phys. Rev.*, 1955, 98, 349.
- (7) Kirczenow G., *Phys. Rev.*, 1985, B31, 5376.
- (8) Alstrom P., *Solid St. Comm.*, 1985, 56, 1047.

SURFACE SPIN RELAXATION OF CURRENT CARRIERS IN GRAPHITE AS A REASON FOR LOW TEMPERATURE PEAK FORMATION IN TEMPERATURE DEPENDENCE OF CONDUCTION ESR LINEWIDTH

A.M. Ziatdinov* and V.V. Kainara

Institute of Chemistry, Far Eastern Branch of the Russian Academy of Sciences.
159, Prosp. 100-letiya, 690022 Vladivostok, RUSSIA. E-mail: chemi@online.ru.

Keywords: graphite, ESR

INTRODUCTION

In all previous investigations of conduction electron spin resonance (CESR) phenomenon in graphite at the analysis of the resonance line shape and linewidth the surface spin relaxation effects were ignored. We have studied the dependence of CESR signal linewidth in highly oriented pyrolytic graphite (HOPG) on temperature and sample dimensions and have shown that the experimental data may be explained well, if the surface spin relaxation of graphite current carriers is taken into consideration.

EXPERIMENTAL

In HOPG investigated the linewidth, at external constant magnetic field $H_0 \parallel c$ (ΔH_c), is as narrow as $\sim 6 \times 10^{-4}$ T near room temperature and first increases remarkably with temperature decrease, and then the rise of ΔH_c with decreasing temperature is followed by a distinct peak at ~ 20 K in a manner similar to that of the g_c -shift (Fig. 1A). At $H_0 \perp a$, the linewidth ($\Delta H_a \sim 5 \times 10^{-4}$ T) also increases with lowering temperature (Fig. 1A), in a manner similar to that of the ΔH_c , despite the fact that g_a -shift does not depend on temperature. The linewidth monotonously depends on the H_0 orientation. While l (HOPG plate width) tends to zero the experimental value of CESR linewidth tends to the infinity (Fig. 1B). (Whereas the corresponding theoretical value calculated with using the well-known Dyson¹ expression for CESR line shape tends to the finite value). At all temperatures the microwave field power and frequency, and the frequency of H_0 modulation had no observable effect on the CESR linewidth.

RESULTS AND DISCUSSION

At the present time there is no consensus among researchers on both the CESR linewidth origin and its temperature dependence.

Kawamura *et al.*² showed that at $H_0 \parallel c$ the Elliot's³ expression for the CESR linewidth for $T \gg \Theta_D$ (Θ_D is the Debye temperature) describes the graphite CESR linewidth temperature dependence in the interval 77-300 K qualitatively at least.

Matsubara *et al.*⁴ considered the temperature variation of graphite CESR linewidth at $H_0 \parallel c$ as a direct consequence of motional narrowing effect in the limit of the incomplete averaging of the line. In this case the g -shift is averaged over all energy states of current carriers, but the linewidth contains the components which are proportional to the square of the microwave frequency.

Kotosonov⁵ pointed out that the small values of CESR linewidth are an evidence for complete averaging of the g -factor over all the energy states of current carriers during the spin-lattice relaxation.

According to the literature data⁶ in graphite the Θ_D is ~ 400 K. Therefore the description of the graphite CESR linewidth temperature dependence by Elliot's³ expression for the $T \gg \Theta_D$ is not correct. Furthermore, this expression does not explain the presence of the linewidth temperature dependence at $H_0 \perp c$ even at a qualitative level since in this orientation of H_0 the value of g -factor does not depend on temperature. The independence of the CESR linewidth on the microwave frequency shows that interpretation of the linewidth temperature dependence as a result of the motional narrowing of the incomplete averaging line also is not correct. The Kotosonov's⁵ point of view does not contradict to the experimental data, but he did not consider the nature of linewidth temperature dependence.

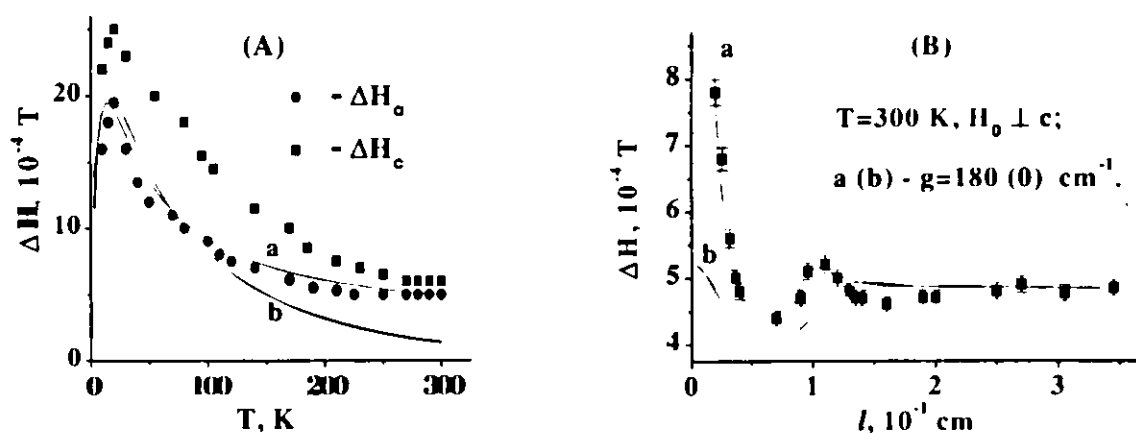


Fig. 1. Graphite CESR linewidth, ΔH , vs. temperature (A) and sample width, l , (B). In (A), the theoretical curve a (b) was calculated with constant value of intrinsic conduction electron spin relaxation time (using the Elliot³ law for $T < \Theta_D$). $g = (3\varepsilon/4\Lambda_s)$ is the Dyson¹ surface spin relaxation parameter (ε is a probability of spin reorientation during the collision of current carriers with the surface and Λ_s is a mean free path of current carriers in a basal plane).

We offer the following version of origin of CESR linewidth temperature dependence in HOPG. The character of temperature dependence of CESR linewidth on l (Fig. 1B) unequivocally specifies the presence of the contribution of surface spin relaxation into total spin relaxation of current carriers in HOPG investigated. Basing on this fact, the temperature dependence of CESR linewidth in HOPG, including the peak formation near 20 K, may be explained by introducing into consideration 1) the effects of surface spin relaxation of current carriers and, additionally, 2) the presence of a small amount of the localized spins ($\sim 1\%$ of the current carrier concentration) with the value of g -factor being nearly equal to that for conduction electrons and 3) complete averaging of g -factors of the conduction electrons and localized spins. The calculations performed within the framework of this model allow to describe experimental data well (Fig. 1A). Note, that the experimental data can be described also well, but with order less concentration of localized spins, if the relaxation of spins on surface of small graphite crystallites in HOPG will be taken into consideration.

This work was partially supported by the Russian Foundation for Basic Research (grant No. 00-03-32610a).

REFERENCES

- (1) Dyson, F.J., Phys. Rev., 1955, 98, 349.
- (2) Kawamura K., Kaneko S., and Tsuzuku T., J. Phys. Soc. Jpn., 1983, 52, 3936.
- (3) Elliot R.J., Phys. Rev., 1954, 96, 266.
- (4) Matsubara K., Tsuzuku T., and Sugihara K., Phys. Rev., 1991, 44, 11845.
- (5) Kotosonov A.S., Carbon, 1988, 26, 189.
- (6) Mizutani V., Kondow T., and Massalski T.B., Phys. Rev., 1978, B17, 3165.

ELECTRICAL CONDUCTIVITY AND CONDUCTION ESR IN INCOMMENSURATE PHASE OF GRAPHITE INTERCALATION COMPOUNDS

A.M. Ziatdinov

Institute of Chemistry, Far Eastern Branch of the Russian Academy of Sciences.
159, Prosp. 100-letiya, 690022 Vladivostok, RUSSIA. E-mail: chemi@online.ru.

Keywords: electrical conductivity, intercalation compounds, ESR

INTRODUCTION

In graphite intercalation compounds (GICs) $C_{5n}HNO_3$ ($n=1,2,3,\dots$) the two-dimensional liquid-like layers of HNO_3 are ordered and form a two-dimensional crystal at temperatures below $T_c \sim 250$ K¹. Layers of HNO_3 may be incommensurate with a carbon net along one of its crystallographic directions and they undergo a structural phase transition of the incommensurate phase - commensurate phase type at $T_{i-c} \sim 210$ K¹. This paper is devoted to the results of the basal plane (σ_a) and the c-axis (σ_c) electrical conductivity studies in incommensurate phase of these compounds.

RESULTS AND DISCUSSION

The measurements of the σ_a - conductivity of $C_{5n}HNO_3$ have been carried out by the contactless Wien bridge method. The measurements of the σ_c - conductivity of GICs investigated have been carried out also by the contactless method with using a CESR technique according to the procedure suggested by Saint Jean and McRae².

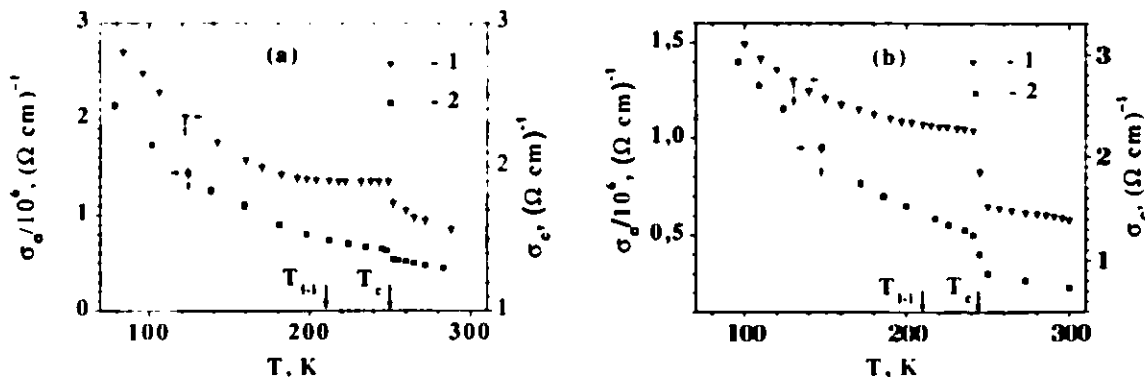


Fig. 1. Temperature dependences of the σ_c (1) - and σ_a (2) - conductivities in 2-nd (a) and 3-rd (b) stage GICs with nitric acid.

For an estimation of the conductivity relaxation time in different phases of GICs investigated in CESR-experiments aimed at determination of σ_c -conductivity, the value of CESR signal linewidth was simultaneously fixed.

Outside the interval of existence of an incommensurate phase of $C_{10}HNO_3$ the σ_a - and σ_c - conductivities increase at decreasing the temperature (Fig. 1a). At the commensurate - incommensurate phase transition both conductivities step-wise increase. Below T_c the σ_a - conductivity continues to increase monotonously, while the temperature dependence of the σ_c - conductivity is absent. The temperature dependence of the σ_c - conductivity is restored only below the "lock-in" phase transition temperature.

In GICs $C_{15}HNO_3$ the changes in σ_a - and σ_c - conductivities are qualitatively identical to those observed in the 2-nd stage compounds (Fig. 1b). However, in the latter case the "plateau" in the temperature dependence of σ_c -conductivity is a less marked one.

In GICs $C_{10}HNO_3$ ($C_{15}HNO_3$) at intercalate crystallization the homogeneously broadened

CESR linewidth undergoes a step-wise increase ~ 3 (~ 1.7) times.

According to Sugihara³ the main contribution to the σ_c - conductivity of the lowest stages ($n = 1+3$) GICs is from the mechanism of a charge transfer through conduction paths (channels). The value of this contribution to the σ_c - conductivity is described as

$$\sigma_c = \frac{16e^2}{\eta^3} m^* d_l V_0^2 \left(\frac{N_c}{\Gamma} \right) \quad (1)$$

where V_0 is the matrix element of the scattering potential, N_c is the number of conduction paths per unit cell, m^* is the effective mass of carriers, d_l is the distance between nearest neighbor layers with an intervening intercalate layer, e is the charge of electron and Γ^* - is a sum of the relaxation rates due to phonon and impurity scattering: $\Gamma = \Gamma_{ph} + \Gamma_I$.

At presence of coupling of the graphite bands across the intercalant, the tight-binding calculations of the c-axis conductivity lead to⁴:

$$\sigma_c \propto K \frac{e^2}{\pi\eta^3} d_l \left(\frac{B^2}{\Gamma} \right), \quad (2)$$

where K includes both numerical and energy-related factors, B is the c-axis interaction energy or resonance integral linking graphite states separated by an intercalate layer.

With neglecting the temperature changes in d_l and V_0 , from Exps. (1) and (2) the conclusion follows that in GICs in some temperature interval σ_c - conductivity can remain constant - at presence of temperature dependence of the σ_a - conductivity, only if within this interval the complete mutual compensation of temperature changes in Γ and B^2 (the band model) or in Γ and N_c (the conduction paths model) takes place. Within the framework of the band model of the σ_c - conductivity in GICs it is not possible to find the physically reasonable mechanism, which could provide the temperature changes in Γ and B required for the constancy of this conductivity. And on the contrary, in the conduction paths model of the σ_c - conductivity it is possible to specify the reason for the ratio N_c/Γ (which determines this conductivity according to Exp. (1)) can be independent on temperature in some GICs phases. Such reason can be high concentration of defects N_d in these phases, when in a first approximation Γ^* is determined only by processes of scattering of current carriers on defects, i. e. $\Gamma^* \cong \Gamma_I^* \propto N_d$. If, besides, $N_c \propto N_d$, it is obvious, that in GIC phases with the high content of defects, the ratio N_c/Γ and, according to Exp. (1), the σ_c - conductivity may be independent on temperature. In such GIC phases any change in N_d directly results in change of σ_a - conductivity. At the same time, the change in N_d can have an effect on the σ_c - conductivity only at its decrease and, moreover, this decrease should be so considerable that contribution of Γ_I to Γ may not be neglected. Thus, it is possible to explain absence of temperature dependence of the σ_c - conductivity in an incommensurate phase of $C_{10}HNO_3$, while temperature dependence for the σ_a - conductivity takes place, by appearance of new structural defects in a sample at the incommensurate crystallization of intercalate, which concentration decreases with temperature decrease. Let us note, that the significant CESR signal broadening (~ 3 times) at the intercalant subsystem crystallization also indirectly confirms the point of view about more defective structure of $C_{10}HNO_3$ in its incommensurate phase.

This work was partially supported by the Russian Foundation for Basic Research (grant No. 00-03-32610a).

REFERENCES

- (1) Dresselhaus M.S., and Dresselhaus D., Adv. Phys., 1981, 30, 139.
- (2) Saint Jean M., and McRae E., Phys. Rev., 1991, B43, 3969.
- (3) Sugihara K., J. Phys. Soc. Jpn., 1993, 62, 624.
- (4) R.S. Markiewicz, Solid St. Commun., 57, 1986, 237.

THE NATURE OF FLUORINE BONDS IN FLUORINATED CARBONS AND XPS STUDIES OF THE GRAPHITE OXIDE INTERCALATION COMPOUNDS WITH DODECAHEDRO-CLOSO-DODECABORIC ACID AND GRAPHITE NITRATE β -C₂₄HNO₃

Yu.M. Nikolenko, V.I. Saldin, N.M. Mishchenko, and A.M. Ziatdinov*
 Institute of Chemistry, Far Eastern Branch of the Russian Academy of Sciences.
 159, Prosp. 100-letiya, 690022 Vladivostok, RUSSIA. E-mail: chemi@online.ru.

Keywords: XPS, fluorinated carbon, intercalation compounds

INTRODUCTION

The possibility of practical application and versatility of properties of graphite intercalation compounds (GIC) maintain interest in their structure and the type of bond between carbon matrix and intercalated species. The structure, bond type and physical properties of the final product of the GIC synthesis depend on the synthesis conditions, reagents and host matrix structure. Modification of the electron structure of graphite matrix leads to the changes in chemical reactivity with guest molecules or ions. This work presents the results of X-ray photoelectron spectroscopy (XPS) investigations of fluorinated graphite oxides (FGO), fluorinated lignin (FL), graphite oxide intercalation compounds with dodecahedro-closo-dodecaboric acid and graphite nitrate (GN) β -C_{8n}HNO₃.

RESULTS AND DISCUSSION

Fluorinated carbons. Previous XPS-investigations of fluorinated carbon fibers (FCF)¹ have shown the possibility of semi-ionic C-F bonds. XPS spectra of graphite fluoride C₂F prepared from graphite-BrF₃ provide evidence for a semi-ionic C-F bond². Fluorination of carbon at temperature $\sim 100^{\circ}$ C and presence of unsaturated C-C bonds in the initial materials define the

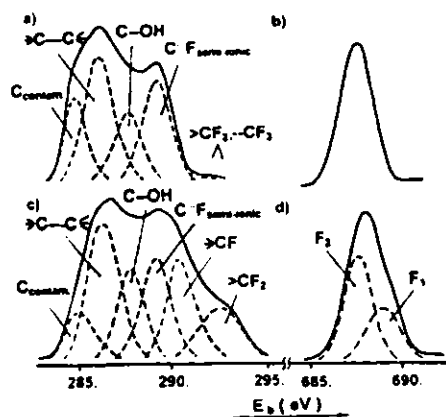


Fig. 1. C1s ('a' and 'c') and F1s ('b' and 'd') XPS spectra of the FGO (a, b) and the FL (c, d).

possibility of a semi-ionic C-F bond formation^{3,4}. For synthesis of FGO using BrF₃ at room temperature we took graphite oxides with different oxygen contents. Details of the FGO synthesis was present in ref.⁵. Fluorination of lignin was carried out with BrF₃ in hydrogen fluoride atmosphere over the temperature range -13° C to -3° C. Structure of initial lignin includes benzoic rings with unsaturated carbon-carbon bonds. The XPS spectra of FL allowed estimation of the importance of a layered structure in the initial substance for synthesis of compounds with semi-ionic carbon-fluorine bonds. Fluorine peaks with binding energies (E_b) equal to 687.6 ± 0.5 eV have been observed in the FGO spectra (Fig. 1b). This value of fluorine E_b is less than usually observed in covalent materials (689.6 ± 0.5 eV) both for aliphatic and cyclic forms⁶. The values of the modified Auger parameter α' of the fluorine XPS

spectra in FGO are 1342.8 ± 0.2 eV and differ from those observed in LiF (1339.8 eV)⁷ and covalent fluorine-carbon compound $-(CF_2-CF_2)_n-$ (1341.2 ± 0.2 eV). Energy E_b of C1s peaks for FGO (Fig. 1a) attributed to semi-ionic C-F bonds is equal to 289.3 ± 0.3 eV. XPS investigation of FL has shown the presence of carbon peaks in the C1s spectra (Fig. 1c)

attributed to semi-ionic C-F bond (289.2 ± 0.2 eV), $>CF$ (290.5 ± 0.2 eV) and $>CF_2$ (292.5 ± 0.2 eV). F1s spectrum of FL (Fig. 1d) includes peaks with $E_b = 687.8 \pm 0.2$ eV (F_2) and 689.2 ± 0.2 eV (F_1). We attribute peak F1 to the covalent C-F bonds and F_2 to the semi-ionic ones. The data reported show that all initial substances for FGO synthesis we used include unsaturated C-C bonds. XPS data on FL show that the layered structure of initial substances is not necessary for the formation of semi-ionic bonds between fluorine and carbon.

Intercalation compounds of graphite oxide with dodecahydro-closo-dodecaboric acid.

The main aims of the synthesis and investigation of the compounds mentioned were to find possibilities to receive chemical and thermal stable non-metal materials of high purity, phase homogeneity and solidity at low specific weight. The boron ceramic compounds such as

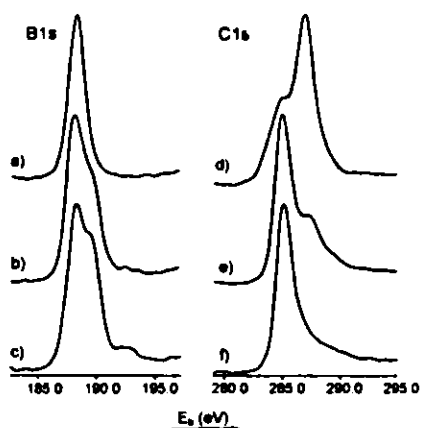


Fig. 1. XPS spectra of the $Cs_2B_{12}H_{12}$ (a), GO (d) and GICs with $B_{12}H_{12}$ (b, e, c, f).

carbide are the materials of this kind. The large interlayer distance in the graphite oxides (GO) defines the choice to use them for synthesis of intercalated compounds with dodecahydro-closo-dodecaboric acid. In Fig. 2 the C1s XPS – spectra of GO (d) and B1s of the model compounds $Cs_2B_{12}H_{12}$ (a) are presented. Intercalation compounds were synthesized at room temperature (Fig. 2 e, b) and then they were heated at $115^\circ C$ during two hours (Fig. 2 f, c). XPS data show that there is an oxidation-reduction reaction between GO and guest molecules. C1s peak of C-O decreases after intercalation and the following heating the samples. Additional peak in the B1s spectra shows the B-O bond in the polymeric form of $B_{12}H_{12}^{2-}$ -anion. The compounds obtained are the hard oxygen containing dodecahydro-closo-dodecaboric polymer with the inert carbon particles having high adhesion

and anticorrosive properties.

Graphite nitrate $\beta-C_{24}HNO_3$. The graphite intercalation compound (GIC) with nitric acid exists in two forms. When the ordinary form, $\alpha-C_{5n}HNO_3$, is exposed to air or N_2 gas for an extended time period, the HNO_3 molecules, which stand essentially perpendicular to the graphite planes, reorient to lie nearly parallel, yielding the more dilute $\beta-C_{8n}HNO_3$ residue compound. We study the composition of the guest molecules layers. The N1s spectrum consists of two peaks, at $406,9 \pm 0.1$ eV and 401.3 ± 0.1 eV. The former one has been attributed to the NO_3 group. The latter has been attributed to the NH_4^+ , resulting from chemical reaction of nitric acid partially reduced to NH_3 with H_3O^+ cation.

This work supported by the Russian Foundation for basic Research (grant No. 00-03-32610)

REFERENCES

- (1) Watanabe N., Nakajima T., and Touhara H., Graphite Fluorides, Elsevier, Amsterdam, 1988, 264P.
- (2) Nazarov A.S., Makotchenko V.G., and Lisitsa V.V., Mat. Sci. Forum (ISIC-6), 1992, 91-92, 10.
- (3) Panich A.M., Bull. Magn. Resonance, 1999, 20, 20.
- (4) Hamwi A., J. Phys. Chem. Solids, 1996, 6-8, 667.
- (5) Tsvetnikov A.K., Nazarenko T. Yu., Matveenko L.A., and Yu.M. Nikolenko Yu. M., Mat. Sci. Forum (ISIC-6), 1992, 91-92, 201.
- (6) Nefedof V.I., X-ray Photoelectron Spectroscopy of Chemical Compounds, Chemistry, Moscow, 1984, 256P.
- (7) Handbook of X-ray Photoelectron Spectroscopy, Perkin-Elmer Corp., U.S.A., 1978, 190P.